Effect of Catalytic Activity on the Metallic Nanoparticle Size Distribution: Electron-Transfer Reaction between $Fe(CN)_6$ and Thiosulfate Ions Catalyzed by PVP−Platinum Nanoparticles

Radha Narayanan and Mostafa A. El-Sayed*

Laser Dynamics Laboratory, School of Chemistry and Biochemistry, Georgia Institute of Technology, Atlanta, Georgia 30332-0400

Received: June 10, 2003; In Final Form: September 5, 2003

The electron-transfer reaction between hexacyanoferrate(III) ions and thiosulfate ions is known to be catalyzed by platinum nanoparticles. In the present study, the stability and catalytic activity of the PVP−Pt nanoparticle during its catalytic function for this electron-transfer reaction is studied. The stability of the nanoparticles after various perturbations was assessed using TEM, and the kinetics of the reaction was followed using absorption spectroscopy. The studies were conducted on four different concentrations of PVP−Pt nanoparticles. It was found that the average size and width of the PVP−Pt nanoparticles decrease slightly after the first and second cycles of the electron-transfer reaction. The size and size distribution width do not change in the presence of only the thiosulfate reactant, whereas the presence of only the hexacyanoferrate reactant results in a reduction of the nanoparticle size. The reduction in the nanoparticle size in the presence of hexacyanoferrate(III) ions is proposed to result from the dissolution of surface Pt atoms through complexation with the strong cyanide ligand. Thiosulfate ions bind to the nanoparticle surface and act as a capping material, resulting in the stability of the nanoparticles. Judging from these observations, it is possible that the mechanism of this catalytic reaction involves the thiosulfate ions binding to the free sites on the surface of the nanoparticles, followed by reaction with hexacyanoferrate ions approaching the nanoparticle surface from the solution. Conducting the reaction with the nanoparticles preexposed to thiosulfate results in very little change in the centers and widths of the size distributions of the nanoparticles, thus suggesting that thiosulfate ions bind to the nanoparticle surface and inhibit desorption of Pt atoms by hexacyanoferrate(III) ions. The kinetics of the electron-transfer reaction during the first and second cycles is similar. The activation energy of the nanoparticle catalytic reaction is found to decrease linearly with increasing nanoparticle concentration during both the first and second cycles. If increasing the nanoparticle concentration leads to more aggregation, then these results suggest that the aggregated Pt has greater catalytic activity than the individual nanoparticles.

Introduction

Because of their large surface-to-volume ratios, nanoparticles offer higher catalytic efficiency per gram than larger-size materials. The field of nanocatalysis has been very active lately, with numerous review articles being published during the past decade in both heterogeneous catalysis, in which the nanoparticles are supported on solid surfaces (e.g., silica or alumina),[1−13] and homogeneous catalysis with colloidal nanoparticles.[14−21] Being small in size is expected to increase the nanoparticle surface tension. This makes surface atoms very active. The question is now raised as to how active they become. Are they active beyond their catalytic function, so that they thus become reactants rather than catalysts? Are they active enough to change their own shape or size during the catalysis?

In the bulk of studies involving catalysis with colloids, TEM characterization of the nanoparticles before and after catalysis is not reported. However, a few studies are available in the literature in which the size distribution of the nanoparticles after recycling, along with the catalytic activity, is reported for characterization. Such studies have been conducted on reactions such as the hydrogenation of ethyl pyruvate,[22] the hydrogenation of arenes,[23] the carbonylation of methanol,[24] the intra- and intermolecular Paulson−Khand reactions,[25] the hydrogenation of alkenes,[26] and the Suzuki reaction between phenylboronic acid and iodobenzene.[27] Some papers have also discussed the catalytic activity of nanoparticles upon recycling, but these works do not examine the stability of the nanoparticles after catalysis. Such studies have been conducted for reactions including the hydrogenation of alkenes,[28] the Heck reaction between aryl halides and *n*-butylacrylate,[29] the hydrogenation of olefins,[30] and the hydrogenation of unsaturated fatty acid esters.[31] In a review article on transition metal colloids,[32] it was pointed out that the major interest of the reusability of nanoparticle catalysts has not been systematically studied or published in the metal colloid literature.

For reactions catalyzed by metal nanoparticles in colloidal solution, very few detailed examinations of the causes of size distribution changes, the effects of various chemicals, and the effects of changes in the nanoparticles on the catalytic activity upon recycling have been published. A detailed examination is necessary to evaluate the nanoparticles' usefulness in catalyses and to understand in detail the mechanism of "nanocatalysis". This will enable a much better understanding of what kind of nanoparticles are best for catalysis and also provide insight into

* To whom correspondence should be addressed. E-mail: mostafa.el-sayed@chemistry.gatech.edu.

10.1021/jp035647v CCC: $25.00
Published on Web 10/21/2003

how to make the nanoparticles more stable and maintain their catalytic activity.

Previously, we conducted a detailed examination of the stability of PVP−Pd nanoparticles catalyzing the Suzuki reaction between phenylboronic acid and iodobenzene.[27] We found that the nanoparticles increased in size after the first cycle of the reaction and decreased in size after the second cycle of the reaction. The increase in the size of the nanoparticles was attributed to Ostwald ripening of the nanoparticles, and the decrease in size after the second cycle was blamed on the aggregation and precipitation of large nanoparticles. The effects of the individual chemicals involved in the reaction were also examined. It was also found that the catalytic activity greatly diminished upon recycling, which is due to a lower number of nanoparticles present in solution because of the larger nanoparticles aggregating and precipitating out of solution and also because of the biphenyl product poisoning the active sites.

The electron-transfer reaction between hexacyanoferrate(III) ions and thiosulfate ions results in the formation of hexacyanoferrate(II) ions and tetrathionate ions. The reaction can even proceed without a catalyst, but it occurs at a very low rate. The electron-transfer reaction has recently been catalyzed using various metal nanoparticles as catalysts. Citrate-capped gold nanoparticles,[33,34] platinum nanoparticles prepared in situ in water-in-oil microemulsions by the aerosol OT (AOT)−water−heptane system,[35] and polyacrylate-stabilized platinum nanoparticles[36] have all been used to catalyze the electron-transfer reaction between hexacyanoferrate(III) ions and thiosulfate ions to form hexacyanoferrate(II) ions and tetrathionate ions.

In this paper, the stability of PVP−Pt nanoparticles after being used to catalyze the electron-transfer reaction between hexacyanoferrate(III) and thiosulfate ions and after recycling for the second cycle was assessed by using TEM to determine whether any changes in the centers and widths of the size distributions of the nanoparticles occurred. The effects of the individual chemicals involved in the reaction on the stability of the nanoparticles were also studied. The catalytic activity of the nanoparticles during the first and second cycles of the reaction was assessed using absorption spectroscopy to follow the kinetics and determine the activation energy.

We found that, after the first and second cycles of the electron-transfer reaction, the centers and widths of the size distributions of the PVP−Pt nanoparticles decreased slightly. The presence of hexacyanoferrate(III) ions resulted in a great reduction in the size of the nanoparticles, which could be due to these ions reacting with the Pt atoms in the nanoparticle surface and dissolving the atoms. The presence of thiosulfate ions results in the nanoparticles maintaining their size, which could be due to these ions binding to the nanoparticle surface. As a result, we propose that the mechanism of the electron-transfer reaction involves thiosulfate ions binding to the nanoparticle surface and reacting with hexacyanoferrate(III) ions in solution. Conducting the reaction with the nanoparticles preexposed to thiosulfate resulted in very little change in the nanoparticle size, suggesting that the binding of the thiosulfate ions onto the nanoparticle surface inhibits the desorption of Pt atoms by hexacyanoferrate(III) ions during catalysis. The kinetics of the reaction were found to be similar in the two cycles, and in both cases, the activation energy was found to decrease linearly with increasing nanoparticle concentration.

Experimental Section

Synthesis of PVP−Pt Nanoparticles. The PVP−Pt nanoparticles were synthesized by the reduction of the Pt^{2+} ions with ethanol, similarly to a method described previously[37−39] except that the K_2PtCl_4 salt was used. A solution containing 15 mL of 2 mM K_2PtCl_4, 21 mL of doubly deionized water, 0.0667 g of PVP, and 4 drops of 1 M HCl was heated. The concentration of Pt^{2+} ions present in the solution was 6×10^{-4} M. When the solution was refluxing, 14 mL of ethanol was added. The solution was refluxed for 3 h, and the resulting colloidal solution was dark brown. A drop of the colloidal solution was placed onto a Formvar-stabilized copper TEM grid, and a JEOL 100C TEM was used to determine the average size of the nanoparticles. From the average size and width of the nanoparticles, the average concentration of PVP−Pt nanoparticles formed was determined to be 13.9 ± 1.9 nM. The concentration was determined using the formula

$$[\text{PVP−Pt nanoparticles}] = \frac{[\text{Pt}^{2+}\text{ ions}]N_A}{V_{NP}/V_{Pt\ atom}}$$

where the subscript NP stands for nanoparticle and V is the volume.

Electron-Transfer Reaction. Four PVP−Pt nanoparticle solutions of lower concentrations were prepared from the stock nanoparticle solution (3.2 ± 0.4, 2.2 ± 0.3, 1.8 ± 0.3, and 1.5 ± 0.2 nM). All of the nanoparticle solutions were adjusted to a pH of 7 by the addition of NaOH. For the electron-transfer reaction between hexacyanoferrate(III) ions and thiosulfate ions, 200 μL of 0.01 M potassium hexacyanoferrate(III) and 200 μL of 0.1 M sodium thiosulfate were added to 2 mL of the PVP−Pt nanoparticles. Because the total volume was 2.40 mL, the final concentrations of the PVP−Pt nanoparticle solutions were 2.7 ± 0.4, 1.9 ± 0.3, 1.5 ± 0.2, and 1.2 ± 0.2 nM, respectively.

Recycling of PVP−Pt Nanoparticles for Second Cycle of Electron-Transfer Reaction. To recycle the nanoparticles, the absorption spectrum was taken to make sure that all of the hexacyanoferrate(III) ions had been consumed, thus signaling that the first cycle of the reaction was over. After the first cycle of the electron-transfer reaction was completed, the second cycle of electron-transfer reaction was initiated by adding 2 μL of 1 M potassium hexacyanoferrate(III) and 2 μL of 1 M sodium thiosulfate to the solution. Because the volume increase was only 4 μL for a total volume of 2.404 mL, the concentrations of the PVP−Pt nanoparticle solutions were about the same as in the first cycle (2.7 ± 0.4, 1.9 ± 0.3, 1.5 ± 0.2, and 1.2 ± 0.2 nM). Because there was negligible difference in the concentrations, the stability and catalytic activity of the nanoparticles can be compared for the first and second cycles. The effect of recycling the catalyst on the stability of the nanoparticles was assessed using TEM, and the kinetics and activation energy of the reaction with the recycled nanoparticles were compared with those obtained during the first cycle by using absorption spectroscopy.

Kinetics of the Electron-Transfer Reaction. The kinetics of the reaction was monitored by using absorption spectroscopy with a Shizmadzu UV−vis−NIR spectrophotometer. The disappearance of the hexacyanoferrate(III) peak as a function of time was monitored by subtracting the absorption at 500 nm from the absorption at 420 nm. At 420 nm, both the hexacyanoferrate(III) ions and the platinum nanoparticles absorb, whereas at 500 nm, only the platinum nanoparticles absorb, and they do so with an absorption coefficient very close to that at 420 nm. The absorbance was monitored every 10 min for 40 min. The slope of the graph of $-\ln A$ vs time gives the rate constant, k. The rate constant of the reaction was determined at four different temperatures (25, 30, 40, and 45 °C) for the four

different concentrations of catalyst. To carry out the reaction at different temperatures, a brass cuvette holder connected with tubes to the ethylene glycol bath was placed inside the spectrophotometer. The quartz cell was placed in the brass holder and heated to the desired temperature. A thermocouple was placed in the brass holder to monitor the temperature throughout the experiment. From the slope of the graph of ln k vs 1000/T, the activation energy of the reaction was determined. The activation energy of the reaction was determined for all four different concentrations of the catalyst for the first and second cycles of the reaction.

Stability of the PVP−Pt Nanoparticles under Various Conditions. The JEOL 100C TEM was used to determine any changes in the center and width of the size distribution of the PVP−Pt nanoparticles after the first and second cycles of the reaction. This was done for all four concentrations of the nanoparticle catalyst. The effect of hexacyanoferrate(III) ions on the PVP−Pt nanoparticles and the effect of thiosulfate ions on the PVP−Pt nanoparticles were also assessed by using TEM to determine whether any changes occurred as a result of the presence of either of the reactants by itself. The absorption spectrum of the nanoparticles in the presence of hexacyanoferrate(III) ions was also followed at 0 min and after 2 days to determine whether any changes in the spectrum occurred. Also, the effect of catalyzing the reaction with PVP−Pt nanoparticles preexposed to thiosulfate ions on the nanoparticle size was examined.

The PVP−Pt nanoparticle samples were spotted by placing a drop of the solution onto a Formvar-stabilized copper grid and allowing the drop to evaporate in air. The spotted samples required approximately 2 h to dry as they are aqueous. Because the same deposition conditions were employed for all of the samples, the evaporation rate of the solvent was fairly reproducible from one sample to another. For each experiment, the internal reproducibility of the observed particle size and distribution was verified by spotting the sample onto three separate TEM grids. Also, TEM images were taken from different sections of the TEM grids to verify the particle size and distribution. The general reproducibility of the observed particle size and distribution was verified by repeating each experiment three times. As a result, it is possible to compare the particle size and distribution changes under the various conditions.

The nanoparticle size and size distribution were determined by counting approximately 1800 nanoparticles from nine enlarged TEM images (approximately 200 nanoparticles from each TEM image). The size distribution plots were fit using a Gaussian model with Microcal Origin 5.0 graphing software to determine the centers and widths of the distributions. The center of a size distribution represents the most probable or average size of the nanoparticles (depending on the shape of the distribution). The width of a size distribution gives an idea of how much the sizes of the nanoparticles vary from the average.

Results and Discussion

Stability of PVP−Pt Nanoparticles. The stability of the PVP−Pt nanoparticles after the first and second cycles of the electron-transfer reaction was investigated. The aim was to determine whether any changes occurred in the center and width of the size distribution of the nanoparticles after the first and second cycles of a mild reaction. The TEM images and Gaussian fits of the size distributions of the 2.7 ± 0.4 nM PVP−Pt nanoparticles for the various conditions are shown in Figures 1 and 2. The results obtained for the other three concentrations of PVP−Pt nanoparticles are very similar to those obtained for the PVP−Pt nanoparticles with a concentration of 2.7 ± 0.4 nM and are summarized in Table 1.

Effects of Catalysis and Recycling. Figure 1a shows a typical TEM image of the PVP−Pt nanoparticles immediately after the addition of the reactants, hexacyanoferrate(III) ions and thiosulfate ions (time = 0). Figure 1b shows the Gaussian fits of the size distributions of the PVP−Pt nanoparticles at time = 0. It can be seen that the PVP−Pt nanoparticles are monodisperse with the centers of distributions at 4.9 ± 0.1 nm and distribution widths of 0.7 ± 0.1 nm. Figure 1c shows a typical TEM image of the PVP−Pt nanoparticles after the first cycle of the reaction, and Figure 1d shows the corresponding Gaussian fits of the size distributions. By comparing the centers and widths of distributions after the first cycle to those before the reaction, it can be seen that there is a 2% decrease in the sizes of the centers and a 14% decrease in the widths of the distributions. The trend of the slight decrease in the size of the nanoparticles after the first cycle of the reaction occurs at all four concentrations of the PVP−Pt nanoparticle catalyst, as shown in Table 1.

Figure 1e shows the TEM images after recycling of the PVP−Pt nanoparticles for a second cycle of the electron-transfer reaction, and Figure 1f shows the corresponding Gaussian fits of the size distributions. By comparing the centers and widths of the distributions with those before the reaction, it can be seen that the values of the centers and widths of the distributions decrease by 4 and 29%, respectively, after the second cycle of the reaction. An explanation for the slight decrease in the size of the nanoparticles is discussed later in the section on the effects of chemicals. This trend of a slight decrease in size after the second cycle is observed for all four concentrations of the PVP−Pt nanoparticles, as shown in Table 1.

Effects of the Individual Reactants on the Nanoparticles. The effects of the presence of individual reactants on the PVP−Pt nanoparticles were also investigated. The effect of exposing the nanoparticles to only thiosulfate ions was investigated. Figure 2a shows a representative TEM image of the PVP−Pt nanoparticles prior to being exposed to thiosulfate ions, and Figure 2b shows Gaussian fits of the size distributions of the nanoparticles. Figure 2c shows a typical TEM image of the PVP−Pt nanoparticles being exposed to thiosulfate ions for 2 days at 25 °C, and Figure 2d shows Gaussian fits of the size distributions of these nanoparticles. It can be seen that the presence of the thiosulfate ions does not affect the centers or the widths of the size distributions of the nanoparticles. This is true for all four concentrations of PVP−Pt nanoparticle catalyst studied, as can be seen in Table 1. The reason the nanoparticles maintain their stability in the presence of the thiosulfate ions might be that the thiosulfate ions bind to the free sites on the nanoparticle surface and act as a capping material. It is well-known in the literature[40−47] that thiosulfate binds to metal surfaces such as silver, cadmium, palladium, nickel, aluminum, zinc, platinum, etc. As a result, it is very logical to propose that the thiosulfate is binding to the free sites of the PVP−Pt nanoparticle surface.

The effect of the presence of hexacyanoferrate(III) ions on the PVP−Pt nanoparticles was also studied. Figure 2e shows a representative TEM image of the PVP−Pt nanoparticles before being exposed to hexacyanoferrate(III) ions. Figure 2f shows the corresponding Gaussian fits of the size distributions of these nanoparticles. Figure 2g shows a typical TEM image of the PVP−Pt nanoparticles after being exposed to hexacyanoferrate-(III) ions for 2 days at 25 °C. Figure 2h shows the corresponding

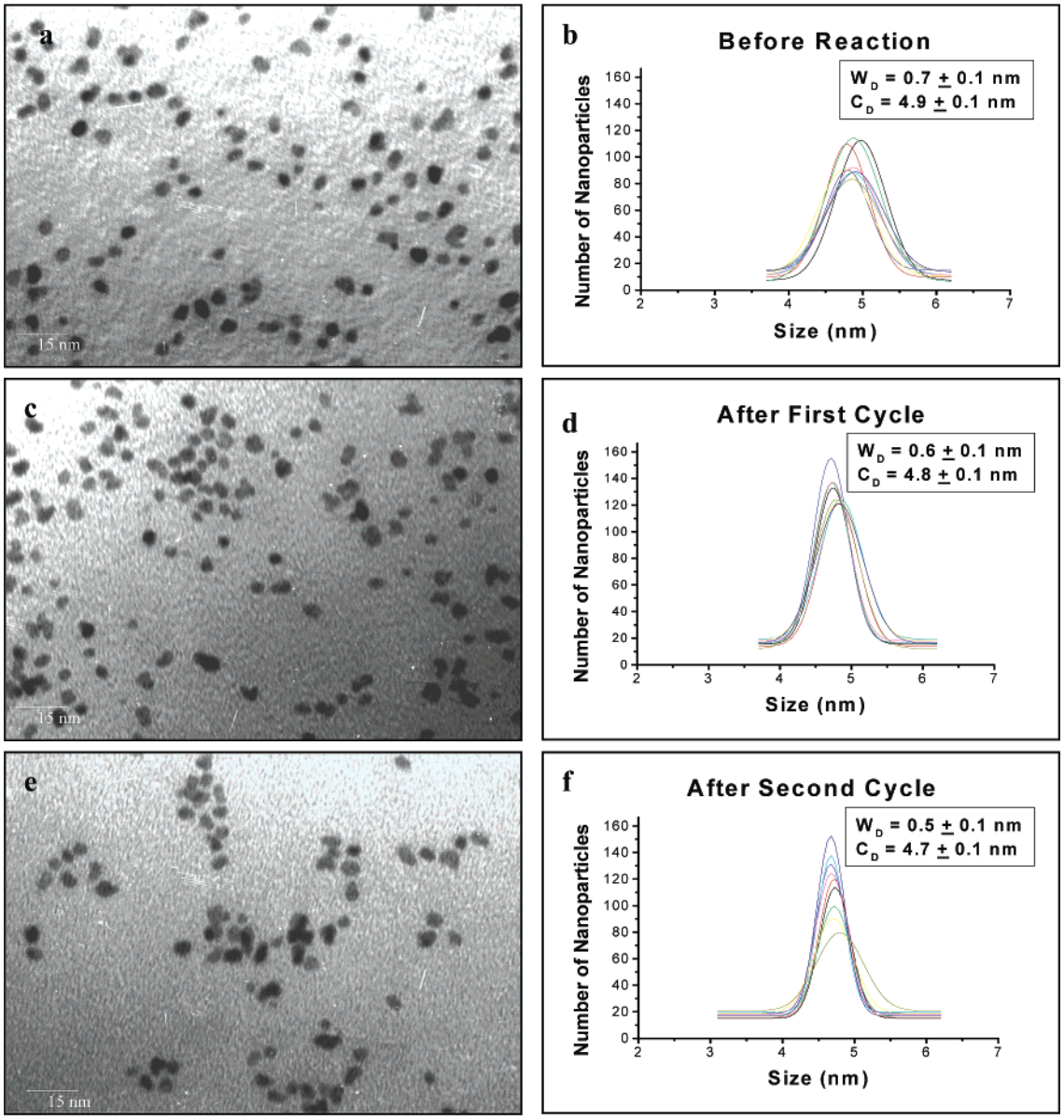

Figure 1. TEM images and Gaussian fits of the size distributions (C_D = center of distribution and W_D = width of distribution) of PVP−Pt nanoparticles (a,b) before the electron-transfer reaction, (c,d) after the first cycle of the electron-transfer reaction, (e,f) and after the second cycle of the electron-transfer reaction.

TABLE 1: Centers and Widths of Gaussian Fits of the Size Distributions of the PVP−Pt Nanoparticles under Various Conditions

	concentration of PVP−Pt NPs (nM)							
	1.2 ± 0.2		1.5 ± 0.2		1.9 ± 0.3		2.7 ± 0.4	
conditions	center (nm)	width (nm)	center (nm)	width (nm)	center (nm)	width (nm)	center (nm)	width (nm)
before first cycle	5.0 ± 0.1	0.7 ± 0.1	4.9 ± 0.1	0.7 ± 0.1	4.9 ± 0.1	0.7 ± 0.1	4.9 ± 0.1	0.7 ± 0.1
after first cycle	4.8 ± 0.1	0.7 ± 0.1	4.8 ± 0.1	0.6 ± 0.1	4.8 ± 0.1	0.7 ± 0.1	4.8 ± 0.1	0.6 ± 0.1
after second cycle	4.7 ± 0.1	0.5 ± 0.1	4.7 ± 0.1	0.5 ± 0.1	4.7 ± 0.1	0.6 ± 0.1	4.7 ± 0.1	0.5 ± 0.1
before exposure to thiosulfate	4.9 ± 0.1	0.8 ± 0.1	4.9 ± 0.1	0.7 ± 0.1	4.9 ± 0.1	0.7 ± 0.1	4.9 ± 0.1	0.8 ± 0.1
after exposure to thiosulfate	4.9 ± 0.1	0.7 ± 0.1	4.9 ± 0.1	0.7 ± 0.1	4.9 ± 0.1	0.7 ± 0.1	4.9 ± 0.1	0.7 ± 0.1
before exposure to hexacyanoferrate(III)	4.9 ± 0.1	0.7 ± 0.1	4.9 ± 0.1	0.7 ± 0.1	4.8 ± 0.1	0.7 ± 0.1	4.9 ± 0.1	0.7 ± 0.1
after exposure to hexacyanoferrate(III)	3.8 ± 0.1	0.6 ± 0.1	3.7 ± 0.1	0.5 ± 0.1	3.8 ± 0.1	0.6 ± 0.1	3.8 ± 0.1	0.6 ± 0.1

Gaussian fits of the size distributions of the exposed nanoparticles. The presence of only the hexacyanoferrate(III) ions causes the nanoparticles to become smaller in size, which can be seen by the shift in the center of the size distribution toward smaller-sized nanoparticles by 22% and the decrease in the width of the size distribution by 14%. This shift in the center of the distributions is evident for all four concentrations of the catalyst, as can be seen in Table 1.

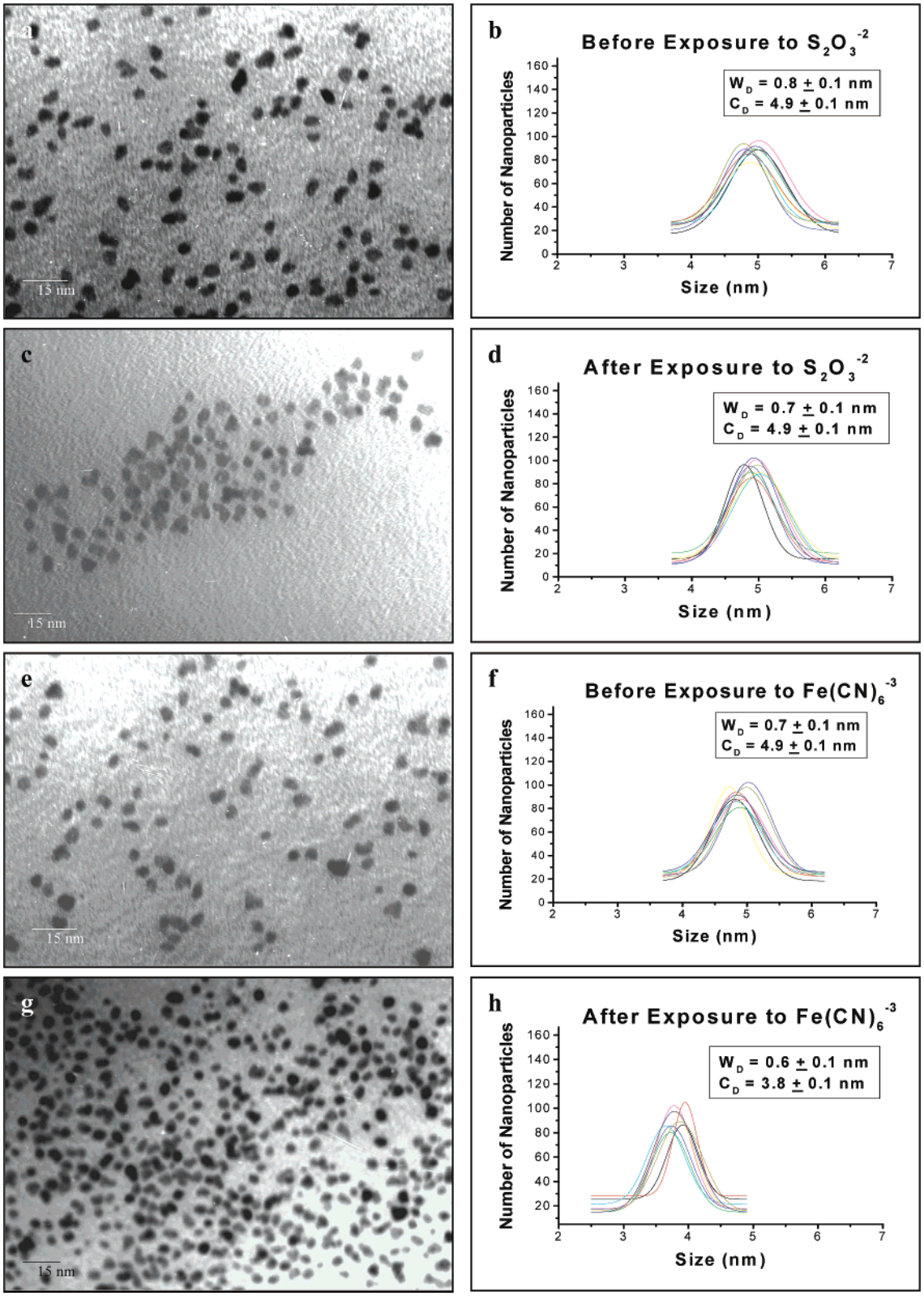

Figure 2. TEM images and Gaussian fits of the size distributions (C_D = center of distribution and W_D = width of distribution) of PVP−Pt nanoparticles (a,b) before exposure to thiosulfate ions [T], (c,d) after exposure to thiosulfate ions [T], (e,f) before exposure to hexacyanoferrate(III) ions [H], and (g,h) after exposure to thiosulfate ions [H].

We propose that the reduction in size is due to the dissolution of surface Pt atoms by complexation with the strong cyanide ligand in hexacyanoferrate(III) ions. The stability constants[48] for $Fe(CN)_6^{-3}$ and $Pt(CN)_4^{-2}$ are 10^{31} and 10^{41}, respectively. Because the stability constant for the platinum complex is much higher than that for the iron complex, it is quite possible that the hexacyanoferrate(III) ions could decomplex and form the more stable platinum complex. To examine this proposal, absorption spectra of hexacyanoferrate(III) ions in the presence of the PVP−Pt nanoparticles were obtained at 0 min and after 2 days. No change in the intensity of the hexacyanoferrate(III) absorption peak at 420 nm was detected. This might be due to a low value of concentration being lost, causing the observed reduction in the size of the nanoparticles in solution. To

TABLE 2: Kinetics (Rate Constants, min^{-1}) of the Electron-Transfer Reaction during the First Cycle

concentration of PVP−Pt nanoparticle solution (nM)	temperature (°C)			
	25	30	40	45
1.2 ± 0.2	0.001 10 ± 0.000 012	0.001 37 ± 0.000 017	0.001 80 ± 0.000 035	0.002 21 ± 0.000 051
1.5 ± 0.2	0.001 23 ± 0.000 051	0.001 64 ± 0.000 035	0.002 13 ± 0.000 104	0.002 60 ± 0.000 101
1.9 ± 0.3	0.001 79 ± 0.000 072	0.002 19 ± 0.000 082	0.002 78 ± 0.000 087	0.003 17 ± 0.000 055
2.7 ± 0.4	0.002 73 ± 0.000 060	0.002 93 ± 0.000 14	0.003 44 ± 0.000 10	0.003 82 ± 0.000 071

TABLE 3: Kinetics (Rate Constants, min^{-1}) of the Electron-Transfer Reaction during the Second Cycle

concentration of PVP−Pt nanoparticle solution (nM)	temperature (°C)			
	25	30	40	45
1.2 ± 0.2	0.001 04 ± 0.000 035	0.001 29 ± 0.000 020	0.001 70 ± 0.000 031	0.002 08 ± 0.000 076
1.5 ± 0.2	0.001 30 ± 0.000 034	0.001 54 ± 0.000 026	0.001 91 ± 0.000 025	0.002 36 ± 0.000 040
1.9 ± 0.3	0.001 69 ± 0.000 054	0.002 08 ± 0.000 035	0.002 64 ± 0.000 057	0.002 93 ± 0.000 051
2.7 ± 0.4	0.002 65 ± 0.000 045	0.002 81 ± 0.000 029	0.003 31 ± 0.000 042	0.003 69 ± 0.000 039

investigate this possibility, we calculated the expected change in the hexacyanoferrate(III) concentration. The concentration of hexacyanoferrate(III) ions that could be lost was calculated in the presence of the highest concentration nanoparticles studied, which is 2.7 ± 0.4 nM. First, the decrease in the volume of one nanoparticle in the solution before and after exposure to hexacyanoferrate(III) ions was calculated using the following formula

$$\Delta V = \frac{4}{3}\pi {r_1}^3 - \frac{4}{3}\pi {r_2}^3$$

where r_1 and r_2 are the radii of the nanoparticle before and after exposure to hexacyanoferrate ions, respectively. Using the density of Pt metal, the atomic volume of platinum was calculated to be 0.0151 nm^3. The number of Pt atoms lost by a nanoparticle was then calculated by dividing ΔV by the atomic volume of the platinum atom and was found to be 2126 atoms per particle. To find the molar concentration of hexacyanoferrate(III) ions lost, the following formula was used

$$\text{molar concentration of hexacyanoferrate(III) ions lost} = (\text{molar concentration of nanoparticles}) \times \frac{2126}{6}$$

On the basis of the reaction stoichiometry, it was assumed that each $Fe(CN)_6^{-3}$ ion dissolves six Pt ions. Thus

$$\text{molar concentration of hexacyanoferrate(III) ions lost} = (\text{molar concentration of nanoparticles}) \times \frac{(2126 \text{ atoms of Pt/nanoparticle})}{(6 \text{ atoms of Pt/molecule of hexacyanoferrate})}$$

This gives 1.0 ± 0.2 μM. The initial concentration of hexacyanoferrate ions present was 833 μM, and as a result, the amount of hexacyanoferrate(III) ions lost was only 0.12% of the initial concentration, which is too small to have been detected.

The small changes in the centers and widths of the distributions after the first and second cycles compared to the large changes occurring in the presence of hexacyanoferrate ions alone could very well result from passivation of the surface by the thiosulfate. The hexacyanoferrate could then react with the thiosulfate, as it could not reach the surface Pt atoms. Judging from the tendency of thiosulfate ions to bind to the nanoparticle surface and to act as a capping agent, we propose that the mechanism of the electron-transfer reaction involves the thiosulfate ions binding to the free metal sites on the surface of the nanoparticles, followed by the reaction with hexacyanoferrate(III) ions approaching the nanoparticle surface from solution.

To test this mechanism, we first exposed the PVP−Pt nanoparticles to thiosulfate ions and then initiated the electron-transfer reaction by the addition of hexacyanoferrate(III) ions. Parts a and b of Figure 3 show a typical TEM image and Gaussian fits of the nanoparticle size distributions before the electron-transfer reaction with preexposed Pt nanoparticles, while parts c and d show a representative TEM image and Gaussian fits of the nanoparticle size distributions after the first cycle of the electron-transfer reaction with the preexposed Pt nanoparticles. Parts e and f of Figure 3 show the TEM image and Gaussian fits of the nanoparticle size distributions after the first cycle of the electron-transfer reaction under normal conditions (repeat of Figure 1c and d) for comparison. It can be seen that very little change occurs in the centers and widths of the size distributions after the reaction with the preexposed nanoparticles, whereas under normal conditions, the size distribution narrows, thus supporting the passivation effect of the preexposed nanoparticles to thiosulfate.

Catalytic Activity of PVP−Pt Nanoparticles during the First and Second Cycles. The kinetics of the electron-transfer reaction with PVP−Pt nanoparticles was followed by absorption spectroscopy in which the disappearance of the hexacyanoferrate(III) ion at 420 nm was monitored as a function of time at different temperatures. The activation energy of the reaction was determined for each of the four concentrations of the catalyst studied in the temperature range between 25 and 45 °C. The kinetics of the reaction was followed at 25, 30, 40, and 45 °C. Tables 2 and 3 present a comparison of the kinetics of the reaction at the four different temperatures at four different concentrations of the catalyst for the first and second cycles.

To follow the kinetics at the second cycle, the reaction was allowed to proceed to completion at room temperature, more fresh reactants were added, and the kinetics were followed at the different temperatures for the second cycle. It can be seen that the kinetics of the reaction during the second cycle is similar to that of the first cycle. This observation is consistent with the finding that very slight changes in the nanoparticle size and its distribution occur and, as a result, the catalytic activity could remain unchanged for the second cycle of the reaction.

It is worth noting that the effect of catalyst concentration on the activation energy of the reaction has not been studied using nanoparticle-based catalysts. However, in homogeneous catalysis (not nanoparticle-based), a few papers have been published[49−55] that discuss the effect of the catalyst concentration on the activation energy of the reaction. Among these studies, some showed that the activation energy was dependent on the catalyst

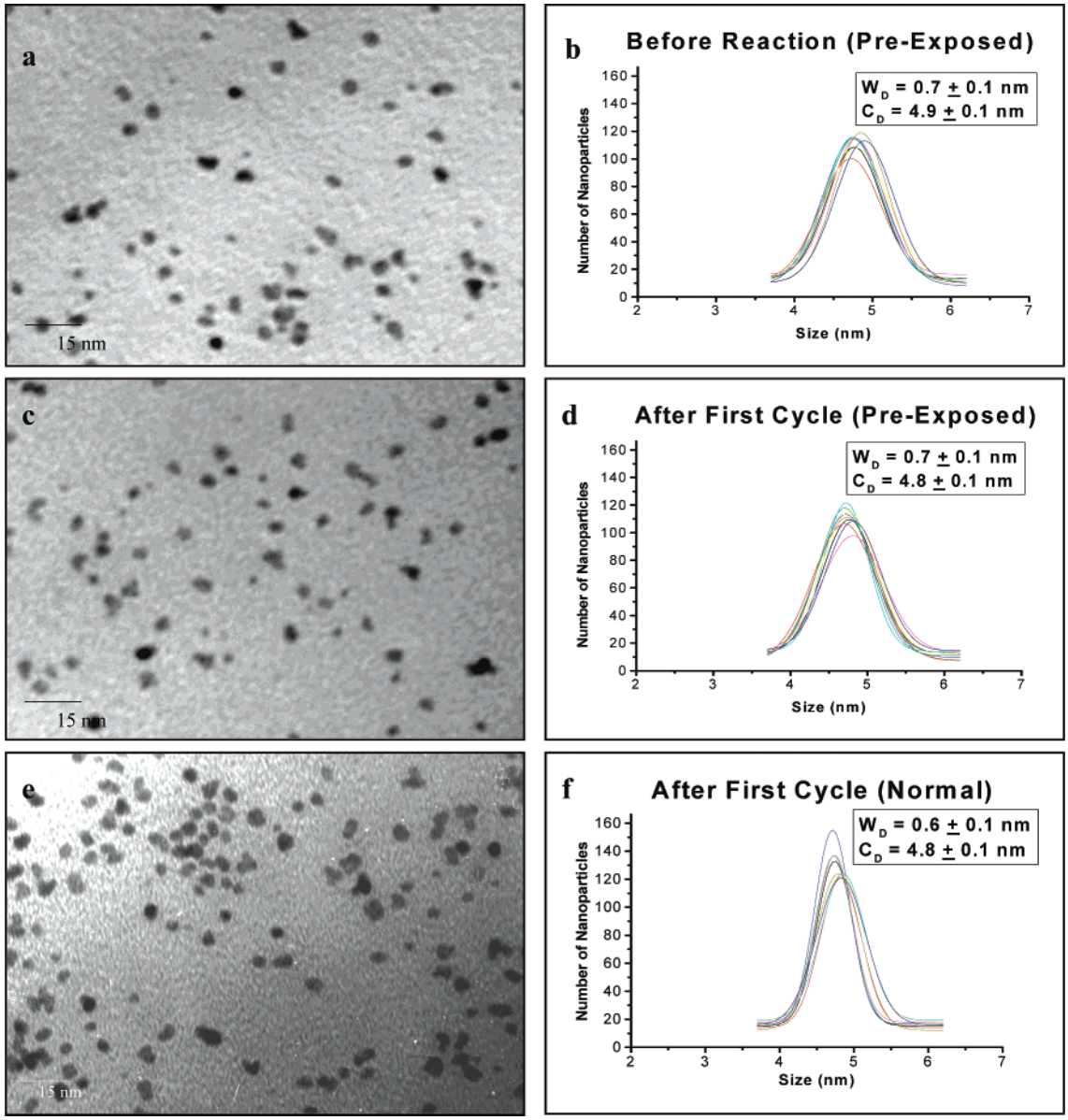

Figure 3. TEM images and Gaussian fits of the size distributions (C_D = center of distribution and W_D = width of distribution) (a,b) before electron-transfer reaction with PVP−Pt nanoparticles preexposed to thiosulfate, (c,d) after first cycle of electron-transfer reaction with PVP−Pt nanoparticles preexposed to thiosulfate, and (e,f) after first cycle of the electron-transfer reaction with PVP−Pt nanoparticles under normal conditions.

concentration, as in the solid-state polycondensation of poly(ethylene terephthalate) catalyzed by antimony trioxide,[49] zinc octoate/nonylphenol-catalyzed thermal cure of bisphenol A dicyanate,[50] and the thermal cure reaction in the presence of various transition metal acetyl acetonates and dibutyl tin dilaurate (DBTDL).[51] In contrast, some showed that the activation energy was independent of the catalyst concentration, as in the reaction of epoxy resin with an acrylic copolymer catalyzed by dimethylbenzolamine,[52] the formation of polyurethanes catalyzed by dibutyltin dilaurate (DBTDL),[53] the reaction of hydroxyl-terminated polybutadiene with isophorone diisocyanate with the ferric tris(acetyl acetonate) (FeAA) catalyst,[54] and the polycyclotrimerization of 4,4′-thiodiphenylcyanate catalyzed by *n*-nonylphenol.[55]

Table 4 compares the activation energy at the different concentrations of the PVP−Pt nanoparticle solutions for the first and second cycles of the electron-transfer reaction. It can be seen that the activation energies for the four concentrations of catalyst during the second cycle are similar to those for the first cycle. Figure 4a shows a plot of the activation energy as a function of the catalyst concentration for the first cycle of the reaction. A very interesting observation is that the activation energy decreases linearly with increasing concentration of the PVP−Pt nanoparticles. Figure 4b shows a plot of the activation energy vs the concentration of the PVP−Pt nanoparticle solution for the second cycle of the reaction. It can be seen that the activation energy also decreases linearly with increasing concentration of PVP−Pt nanoparticles for the second cycle. The changes in the activation energy are similar for the two cycles of the reaction.

TABLE 4: Activation Energies for the Electron-Transfer Reaction for the First and Second Cycles

concentration of PVP−Pt nanoparticle solution (nM)	activation energy (kJ/mol)	
	first cycle	second cycle
1.2 ± 0.2	25.3 ± 2.1	24.2 ± 1.3
1.5 ± 0.2	22.6 ± 1.2	22.2 ± 1.6
1.9 ± 0.3	20.5 ± 0.8	20.0 ± 1.6
2.7 ± 0.4	12.4 ± 0.8	13.3 ± 0.9

The observed decrease in the activation energy can only be explained if the nature of the catalytic particles changes with

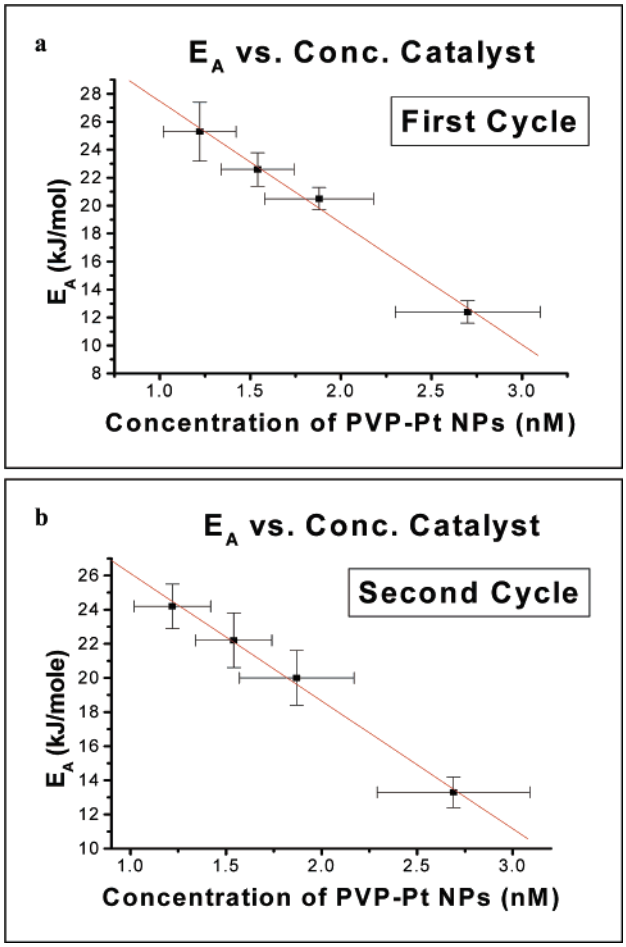

Figure 4. Plot of activation energy (E_A) as a function of catalyst concentration (a) during the first cycle of the electron-transfer reaction and (b) during the second cycle of the electron-transfer reaction.

concentration. One important change that is known to occur in colloidal nanoparticle solutions is aggregation. As a result, the type of catalytic particles changes as new sites created at the intersection of the aggregated nanoparticles are formed. It is possible that atoms at these sites are more active catalytically, thereby giving rise to a reduction in the activation energy. The mechanism of the reaction involves thiosulfate ions binding to the active sites of the nanoparticles and hexacyanoferrate ions approaching the nanoparticle surface from the solution.

Conclusions

PVP−Pt nanoparticles decrease greatly in size if mixed with only hexacyanoferrate(III) ions, but they are not affected if mixed with only thiosulfate ions and decrease slightly in size during the reaction between hexacyanoferrate(III) ions and thiosulfate ions. These results suggest that the hexacyanoferrate-(III) ions alone dissolve the Pt from the nanoparticle surface to form a cyano complex, as expected from thermodynamic considerations. Thiosulfate seems to bind to the surface, thus passivating it against attack by the hexacyanoferrate, which, instead, reacts with the surface-bound thiosulfate to give the reaction products.

The kinetics of the reaction during the second cycle of the electron-transfer reaction is similar to that of the first cycle. In both cycles, the activation energy of the reaction decreases linearly with increasing concentration of the nanoparticle solution. If increasing concentration leads to more aggregation, these results suggest that aggregated Pt nanoparticles have a higher catalytic activity than individual nanoparticles.

Acknowledgment. We thank the National Science Foundation (CHE-0240380) for funding of this research. We also thank the Electron Microscopy Center for the JEOL 100C TEM facility, which we used to perform the TEM experiments.

References and Notes

(1) Eppler, A.; Rupprechter, G.; Guczi, L.; Somorjai, G. A. *J. Phys. Chem. B* **1997**, *101* (48), 9973.
(2) Toshima, N.; Yonezawa, T. *New J. Chem.* **1998**, *22* (11), 1179.
(3) Schmid, G. *Met. Cluster Chem.* **1999**, *3*, 1325.
(4) Puddephatt, R. J. *Met. Cluster Chem.* **1999**, *2*, 605.
(5) Henry, C. R. *Appl. Surf. Sci.* **2000**, *164*, 252.
(6) St. Clair, T. P.; Goodman, D. W. *Top. Catal.* **2000**, *13* (1, 2), 5.
(7) Kralik, M.; Corain, B.; Zecca, M. *Chem. Pap.* **2000**, *54* (4), 254.
(8) Chusuei, C. C.; Lai, X.; Luo, K.; Goodman, D. W. *Top. Catal.* **2001**, *14* (1−4), 71.
(9) Bowker, M.; Bennett, R. A.; Dickinson, A.; James, D.; Smith, R. D.; Stone, P. *Stud. Surf. Sci. Catal.* **2001**, *133*, 3.
(10) Kralik, M.; Biffis, A. *J. Mol. Catal. A: Chem.* **2001**, *177* (1), 113.
(11) Thomas, J. M.; Raja, R. *Chem. Rec.* **2001**, *1* (6), 448.
(12) Mohr, C.; Claus, P. *Sci. Prog.* **2001**, *84* (4), 311.
(13) Thomas, J. M.; Johnson, B. F. G.; Raja, R.; Sankar, G.; Midgley, P. A. *Acc. Chem. Res.* **2003**, *36* (1), 20.
(14) Bradley, J. S. *Clusters Colloids* **1994**, 459.
(15) Duff, D. G.; Baiker, A. *Stud. Surf. Sci. Catal.* **1995**, *91*, 505.
(16) Toshima, N. *NATO ASI Ser., Ser. 3* **1996**, *12*, 371.
(17) Boennermann, H.; Braun, G.; Brijoux, G. B.; Brinkman, R.; Tilling, A. S.; Schulze, S. K.; Siepen, K. *J. Organomet. Chem.* **1996**, *520* (1−2), 143.
(18) Fugami, K. *Organomet. News* **2000**, *1*, 25.
(19) Mayer, A. B. R. *Polym. Adv. Technol.* **2001**, *12* (1−2), 96.
(20) Bonnemann, H.; Richards, R. *Syn. Meth. Organomet. Inorg. Chem.* **2002**, *10*, 209.
(21) Moiseev, I. I.; Vargaftik, M. N. *Russ. J. Chem.* **2002**, *72* (4), 512.
(22) Collier, P. J.; Iggo, J. A.; Whyman, R. *J. Mol. Catal. A: Chem.* **1999**, *146* (1−2), 149.
(23) Sculz, J.; Roucoux, A.; Patin, H. *Chem. Eur. J.* **2000**, *6* (4), 618.
(24) Wang, Q.; Liu, H.; Han, M.; Li, X.; Jiang, D. *J. Mol. Catal. A: Chem.* **1997**, *118* (2), 145.
(25) Kim, S.; Son, S. U.; Lee, S. S.; Hyeon, T.; Chung, Y. K. *Chem. Commun.* **2001**, 2212.
(26) Larpent, C.; Menn, B. F.; Patin, H. *J. Mol. Catal.* **1991**, *65*, L35.
(27) Narayanan, R.; El-Sayed, M. A. *J. Am. Chem. Soc.*, **2003**, *125* (27), 8340.
(28) Chechik, V.; Crooks, R. M. *J. Am. Chem. Soc.* **2000**, *122*, 1243.
(29) Yeung, L. K.; Crooks, R. M. *Nano Lett.* **2001**, *1* (1), 14.
(30) Dupont, J.; Fonseca, G. S.; Umpierre, A. P.; Fichtner, P. F. P.; Teixeira, S. R. *J. Am. Chem. Soc.* **2002**, *124*, 4228.
(31) Hirai, H.; Chawanya, H.; Toshima, N. *Nippon Kagaku Kaishi* **1984**, *6*, 1027.
(32) Roucoux, A.; Schulz, J.; Patin, H. *Chem. Rev.* **2002**, *102*, 3757.
(33) Freund, P. L.; Spiro, M. *J. Phys. Chem.* **1985**, *89*, 1074.
(34) Freund, P. L.; Spiro, M. *J. Chem. Soc., Faraday Trans.* **1986**, *82*, 2277.
(35) Clint, J. H.; Collins, I. R.; Williams, J. A.; Robinson, B. H.; Towey, T. F.; Cajean, P.; Khan-Lodhi, A. *Faraday Discuss.* **1993**, *95*, 219.
(36) Li, Y.; Petroski, J.; El-Sayed, M. A. *J. Phys. Chem. B* **2000**, *104*, 10956.
(37) Li, Y.; Hong, X. M.; Collard, D. M.; El-Sayed, M. A. *Org. Lett.* **2000**, *2* (15), 2385.
(38) Li, Y.; Boone, E.; El-Sayed, M. A. *Langmuir* **2002**, *18*, 4921.
(39) Teranishi, T.; Miyake, M *Chem. Mater.* **1998**, *10*, 594.
(40) Ong, C. G.; Leckie, J. O. *Adsorpt. Met. Geomedia* **1998**, 317.
(41) Baggio, S.; Pardo, M. I.; Baggio, R.; Garland, M. T. *Acta Crystallogr. C: Cryst. Struct. Commun.* **1997**, *53* (6), 727.
(42) Rizov, I.; Ilcheva, L *Analyst* **1995**, *120* (6), 1651.
(43) Aruga, R. *Inorg. Chem.* **1978**, *17* (9), 2503.
(44) Cusomano, M.; Giannetto, A.; Cavasino, P. F.; Sbriziolo, C. *Inorg. Chim. Acta* **1992**, *201* (1), 49.
(45) Itabashi, E. *Chem. Lett.* **1978**, *2*, 211.
(46) Foye, W. O., Hu, J, *J. Pharm. Sci.* **1979**, *68* (2), 202.
(47) Foye, W. O.; Kaewchansilp, V. **1979**, *68* (9), 1131.
(48) Sillen, L. S.; Martell, A. E. *Stability Constants of Metal-Ion Complexes*; Metcalfe & Cooper Limited: London, 1964.
(49) Duh, B. *Polymer* **2002**, *43*, 3147.

(50) Mathew, D.; Nair, C. P. R.; Krishnan, K.; Ninan, K. N. *J. Polym. Sci. A: Polym. Chem.* **1999**, *37* (8), 1103.
(51) Catherine, K. B.; Krishnan, K.; Ninan, K. N. *J. Therm. Anal. Calorim.* **2000**, *59* (1−2), 93.
(52) Chu, F.; McKenna, T.; Lu, S. *Eur. Polym. J.* **1997**, *33* (6), 837.
(53) Mayr, A. E.; Cook, W. D.; Edward, G. H.; Murray, G. J. *Polym. Int.* **2000**, *49* (3), 293.
(54) Nair, C. P. R.; Gopalakrishnan, C.; Ninan, K. N. *Polym. Polym. Compos.* **2001**, *9* (8), 531.
(55) Lin, R. H.; Hong, J. L.; Su, A. C. *Polymer* **1995**, *36* (17), 3349.